

High-order nonlinear disturbance observer based zero-bias control for a magnetic suspended system

Rong Hai^a, Zhou Kai^a, Mao Feilong^a

^a Department of Mechanical Engineering, Tsinghua University, ShuangQing Road No.30, Beijing, China, rongh14@mails.tsinghua.edu.cn

Abstract—In this paper, the zero-bias control method is proposed to remove the bias current/flux for the active magnetic bearing (AMB), which is meaningful to decrease the power consumption. The AMB system becomes a high nonlinear system under the zero-bias current controlled mode. Besides, the AMB suffers from lumped uncertainty including parameter uncertainty and external load, which is usually undeterminable and varying. The nonlinear disturbance observer based sliding mode control is proposed to realize the close-loop control of the whole system. Under this control framework, the structure of the controller for a nonlinear system suffered from disturbance can be divided into two parts. One is the normal sliding mode control part to achieve basic performance for the nonlinear system. The other is the compensate part to eliminate the effects caused by the unknown disturbance via disturbance observer. Compared with the methods adopting inner adaptive laws to estimate disturbance such as the adaptive backstepping sliding mode control, the nonlinear disturbance observer has much higher converging rate, which is meaningful for anti-disturbance. Mostly the nonlinear disturbance observer is adopted with the assumption that the derivative of disturbance is approximately equal to zero. In this paper, the disturbance is considered to be time varying, hence the conventional nonlinear disturbance observer is not well suited. Then the high-order nonlinear disturbance observer estimates the disturbance and its derivatives simultaneously, is proposed to handle the time varying disturbance. Under different kinds of disturbance, the high-order nonlinear disturbance observer based sliding mode control method is compared with the sliding mode control, the adaptive backstepping sliding mode control and the conventional nonlinear disturbance observer based sliding mode control. The effectiveness of the proposed high-order disturbance observer based approach for a zero-bias current controlled AMB system is verified by the simulation and experiment results.

Keywords: Zero-bias control, active magnetic bearing, sliding mode control, nonlinear disturbance observer, time-varying disturbance

I. PAPER TEXT

A. Introduction

Due to the promising advantages such as high speed, no friction, absence of lubrication and long lifetime, active magnetic bearing (AMB) has been widely applied in numerical control (NC) machine, flywheels, vacuum pumps, turbos, gyros [1-5].

As well known, one of the main characteristics of AMB system is nonlinearity. The AMB can be controlled by two kinds of ways: the bias controlled way and the zero-bias controlled way. To handle the high nonlinearity in AMB system, the conventional bias controlled way uses the Taylor series expansion to linearize it. However, it brings bias current or bias flux, which intensifies copper losses and rise in temperature [6]. The decreased precision brought by temperature rise is fatal in applications such as NC machine tools. Recently, designs adopting the permanent magnets or utilizing the superconducting technology to generate the bias flux have been proposed, however, it brings problems in installing the permanent magnets or needs extended cooling system. Zero-bias controlled mode which is also called switch control, is therefore proposed to minimize the power consumption for AMB system [6-10]. Only one in a pair of coils has current flow at any given time while current of the other coil is zero under the zero-bias controlled way. Installing the flux sensors in the stator of the AMB to detect flux directly is cost and more complicated than current control with position and current feedback [8]. Therefore, zero-bias current control method is adopted in this work. However, since the AMB system is treated as a high nonlinear system in the zero-bias current controlled way, it is difficult to design a good controller to suspend the rotor of the AMB well, especially under parameter uncertainty and external load (defined as lumped disturbance). Besides, the lumped disturbance is time-varying and undeterminable, which also adds difficulty to the design of controller. Therefore, it is a challenging task to achieve perfect performance for the zero-bias current controlled AMB system.

Much attention has been paid to the sliding mode control (SMC) in the last two decades, due to the advantages of good transient response and good performance to subdue the system uncertainty and the external disturbance [11]. SMC has been applied in many practical systems such as electrical motors [12], magnetic suspended system [13], fluid power electrohydraulic actuator system [14], servopneumatic system [15]. However, SMC method is short of dealing with disturbance with unknown bound. The adaptive sliding mode control (ASMC) method has been proposed to control a magnetic suspended system suffered from unknown disturbance [16]. The adaptive backstepping sliding mode control (ABSMC) technology is used to control permanent magnet synchronous motor suffered from unknown friction force [17] or a new kind of ball and plate system under

disturbance with unknown upper bound [18]. Adaptive laws are designed in the ASMC and ABSMC methods to estimate the disturbance, however, it estimates the disturbance simply via an integral of the sliding mode variable, which asymptotically converges in a relatively slow way.

Disturbance observer based control (DOBC) approach, which combines the disturbance observer with basic control method, attracts much more attention and becomes one of the most popular disturbance rejection method [19]. Under this control framework, the structure of the controller for a nonlinear system suffered from disturbance can be divided into two parts. One is the normal control part to achieve basic performance for the nonlinear system. The other is the compensate part to eliminate the effects caused by the unknown disturbance via disturbance observer. The DOBC method has been used in various applications, [20] and [21] apply the disturbance observer based LQR and SMC respectively on the control of a MAGLEV suspension system, [22] uses the disturbance observer based SMC to the control of a human-driven knee joint, the nonlinear disturbance observer also has been applied in the attitude control of spacecraft [23, 24]. However, an assumption that the disturbance does not change rapidly is made in the above applications, which limits the usage of the controller to the system under the quickly varying disturbance. And the nonlinear disturbance observer is defined as conventional nonlinear disturbance observer (CNDO). The controller combines SMC with disturbance observer is proposed to control the serial flexible joint plant without making that assumption [25]. [4, 26] propose the state-space disturbance observer to deal with the disturbance, however, it is based on the LMI design. Recently, researches about the applications of some kinds of high-order nonlinear disturbance observer to handle high-order disturbance of which the derivatives do not equal to zero have been presented [27-30], however, most are complicated and only the simulation results are given.

In this paper, a nonlinear control system for the zero-bias current controlled AMB system under high-order disturbance is considered. The zero-bias current controlled way is proposed to achieve the power-minimizing control for the AMB, which means the controlled plant is a highly nonlinear one. Besides, the rotor of the AMB suffered from unknown parameter uncertainty and external load. Therefore, the DOBC design that consists of the SMC and nonlinear disturbance observer (NDO) is proposed. The baseline SMC controller is designed to maintain the nominal performance of the zero-bias current AMB without the disturbance, and the function of NDO is to estimate the disturbance and compensate it. The contribution of this paper can be summarized as: (1) A new dynamic model of a zero-bias current controlled AMB system considering the parameter uncertainty and external load, is proposed in this paper. The new model is a highly nonlinear one and the disturbance is considered to be unknown and time-varying. (2) The DOBC design combines the SMC and NDO is applied to the control of the zero-bias current AMB system under unknown disturbance. The deviation of rotor caused by disturbance can be eliminated by the NDO well. (3) A high-order nonlinear disturbance observer (HONDO) combined with SMC is proposed to handle the rapidly changing disturbance. The derivative of disturbance is also estimated by the HONDO. To make a comparison, the CNDO is also used to handle

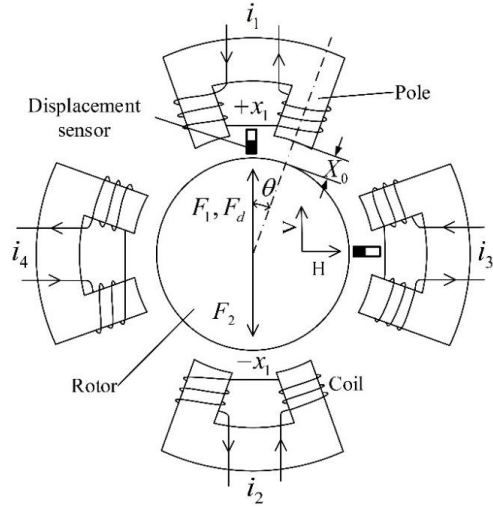


Figure 1. The schematic drawing of the radial heteropolar AMB system.

disturbance. Simulation and experiment results significantly show better performance for the HONDO based design than the CNDO based design in disturbance rejection.

The paper is organized as follows: Section B focuses on the system modeling and description; Section C provides the the SMC design and the HONDO design, the output expressions of controller and stabilized proof are also given; simulation results and some comments are provided in Section D; Section E shows the experiment platform and the corresponding experiment results; Conclusions are given in Section F.

B. Dynamic model of a zero-bias AMB system

The radial heteropolar AMB system with eight magnet poles is researched in this work, as presented in Fig. 1. Eight electromagnet poles are arranged around the rotor symmetrically and can be divided into two pairs in the horizontal and vertical axes. In the zero-bias control configuration, only one in a pair of electromagnet poles works at any time for both axes. Once the coil of the electromagnet pole is energized, an attractive force is generated between the pole and rotor. The motion of rotor can be regulated by controlling the current of coils.

The dynamical model of the radial AMB in the vertical axis is [1]

$$\begin{aligned} M\ddot{x}_1 &= \frac{K_1 i_1^2}{(X_0 - x_1 / \cos \theta)^2} - \frac{K_2 i_2^2}{(X_0 + x_1 / \cos \theta)^2} + F_d' \\ F_d' &= \frac{\Delta K_1 i_1^2}{(X_0 - x_1 / \cos \theta)^2} - \frac{\Delta K_2 i_2^2}{(X_0 + x_1 / \cos \theta)^2} + F_d \end{aligned} \quad (1)$$

$$K_1 = \mu_0 N_1^2 A_{a1} \cos \theta / 4, K_2 = \mu_0 N_2^2 A_{a2} \cos \theta / 4$$

Where K_1 and K_2 are the magnetic force coefficients. ΔK_1 and ΔK_2 represent the parameter uncertainties. F_d is the external force applied to the rotor. F_d' represents the lumped disturbance, including the parameter uncertainties and external force. μ_0 is the magnetic field constant in vacuum ($=4\pi \times 10^{-7} \text{ Vs/Am}$), N_1 , N_2 are the number of the coil turns, A_{a1} , A_{a2} are the areas of the electromagnet poles, i_1 , i_2 are the currents of coils, X_0 is the nominal air gap between the electromagnet pole and the rotor,

x_1 is the displacement of rotor in the vertical direction, θ is the angle between the magnetic pole and vertical axis.

Then a new dynamic model of a zero-bias current controlled one-DOF AMB system can be defined as

$$\begin{aligned} \dot{x}_1 &= x_2 \\ \dot{x}_2 &= ([K_1\alpha_1(x_1) \quad -K_2\alpha_2(x_1)] \begin{bmatrix} I_1 \\ I_2 \end{bmatrix} + F'_d) / M \\ y &= x_1 \\ \alpha_1(x_1) &= 1 / (X_0 - x_1 / \cos \theta)^2 \\ \alpha_2(x_1) &= 1 / (X_0 + x_1 / \cos \theta)^2 \end{aligned} \quad (2)$$

Where $I_1 = i_1^2$ and $I_2 = i_2^2$ are the control inputs, x_1 and x_2 represent the displacement and velocity of the rotor separately, y denotes the output of the system. It can be indicated that there are two control outputs whereas only one input, which is not desired, therefore, the switching laws is defined as

$$\begin{aligned} I_2 = I, I_1 = 0, \alpha(x_1) = -\alpha_2(x_1), K = K_2, \quad x_1 \geq 0 \\ I_1 = I, I_2 = 0, \alpha(x_1) = \alpha_1(x_1), K = K_1, \quad x_1 < 0 \end{aligned} \quad (3)$$

C. Controller design

Inspired by [30], firstly rewrite (2) as follows

$$\begin{aligned} \dot{x}_1 &= x_2 \\ \dot{x}_2 &= g(x_1)I + d \\ y &= x_1, \end{aligned} \quad (4)$$

where $g(x_1) = Ka(x_1) / M$, I is the output of the controller and needed to design, d represents the lumped disturbance, $d = F'_d / M$.

Before the controller design, firstly, define the tracking error and its derivative as

$$\begin{aligned} e &= x_1 - x^* \\ \dot{e} &= \dot{x}_1 - \dot{x}^* \\ \ddot{e} &= \ddot{x}_1 - \ddot{x}^* = g(x_1)I + d - \ddot{x}^*, \end{aligned} \quad (5)$$

where x^* , \dot{x}^* , \ddot{x}^* are the reference position, velocity and acceleration of the rotor respectively.

Let $\phi = [\phi_1 \quad \phi_2]^T = [e \quad \dot{e}]^T$, then (5) can be written into a state-space form as

$$\dot{\phi} = \begin{bmatrix} \phi_2 \\ g(x_1)I - \ddot{x}^* \end{bmatrix} + \begin{bmatrix} 0 \\ 1 \end{bmatrix} d \quad (6)$$

Define $G_d = [0 \quad 1]^T$ and

$$\varphi = \begin{bmatrix} \phi_2 \\ g(x_1)I - \ddot{x}^* \end{bmatrix} = \begin{bmatrix} \varphi_1 \\ \varphi_2 \end{bmatrix}, \quad (7)$$

then system (6) can be written as

$$\dot{\phi} = \varphi + G_d d \quad (8)$$

According to SMC theory [11], there are two steps to design the control system. At first, a sliding surface with desired performance is defined; then, a suitable control law is constructed to drive system states to the sliding surface and remain on it. The SMC algorithm is described as follows.

Firstly, a sliding mode surface is defined as

$$\sigma = [c \quad 1]\phi = c\phi_1 + \phi_2, \quad (9)$$

where c is a positive constant.

The time derivative of σ is

$$\dot{\sigma} = c\dot{\phi}_1 + \dot{\phi}_2 = g(x_1)I - \ddot{x}^* + d + c\dot{e} \quad (10)$$

Based on the reaching law of SMC, the output of controller can be as

$$I = \frac{1}{g(x_1)}[\ddot{x}^* - c\dot{e} - h\sigma - k \operatorname{sgn}(\sigma) - d], \quad (11)$$

where h, k satisfy, $h > 0$ and $k > 0$.

Define a Lyapunov function as follow

$$V_1 = \frac{1}{2}\sigma^2, \quad (12)$$

the time derivative of V_1 is

$$\begin{aligned} \dot{V}_1 &= \sigma\dot{\sigma} \\ &= \sigma(\ddot{x}^* - c\dot{e} - h\sigma - k \operatorname{sgn}(\sigma) - d - \ddot{x}^* + d + c\dot{e}) \\ &= -h\sigma^2 - k\sigma \operatorname{sgn}(\sigma) \\ &\leq 0 \end{aligned} \quad (13)$$

Clearly, it can be concluded that if the lumped disturbance d is known, the sliding mode surface $\sigma = 0$ is always reachable, the control system is therefore stable. Nevertheless, as mentioned above, the lumped disturbance is unmeasurable, which means that an extended disturbance observer is needed to estimate d . Define \hat{d} to be the estimation of the lumped disturbance, then the output of controller take the new form as

$$I = \frac{1}{g(x_1)}[\ddot{x}^* - c\dot{e} - h\sigma - k \operatorname{sgn}(\sigma) - \hat{d}] \quad (14)$$

Define $\tilde{d} = d - \hat{d}$ to be the estimation error, then the time derivative of V_1 becomes

$$\begin{aligned} \dot{V}_1 &= \sigma\dot{\sigma} \\ &= \sigma(\ddot{x}^* - c\dot{e} - h\sigma - k \operatorname{sgn}(\sigma) - \hat{d} - \ddot{x}^* + d + c\dot{e}) \\ &= -h\sigma^2 - \sigma(k \operatorname{sgn}(\sigma) + \tilde{d}) \\ &\leq -h\sigma^2 - \sigma(k \operatorname{sgn}(\sigma) - |\tilde{d}|) \end{aligned} \quad (15)$$

As shown in (15), if $k > |\tilde{d}|$, then $\dot{V}_1 \leq 0$ can be held. Therefore, the sliding mode surface $\sigma = 0$ is reachable and the stability of the whole system is proven.

Remark 1: From above, it can be known that the value of k can be greatly decreased (k only needs to be greater than $|\tilde{d}|$) as long as the \hat{d} matches the unknown lumped disturbance well, while k needs to be greater than $|d|$ in the conventional SMC design [11], which is helpful to alleviate the chattering phenomenon. Therefore, a well designed disturbance observer is required to track the disturbance. Then, it follows the disturbance observer design parts.

In order to handle the varying disturbance, a high-order nonlinear disturbance observer is proposed, which observes the disturbance as well as its derivatives. For the convenience of realization, the zero/first/second order derivatives of disturbance are considered here, and an assumption is made that the feasibility of HONDO is existing if only the lumped disturbance meets the following assumption:

Assumption: The lumped disturbance d and its first two-order derivatives are continuous and bounded, namely

$$\left| \frac{\partial^j d(t)}{\partial t^j} \right| \leq \mu, \quad \text{for } j = 0, 1, 2 \quad (16)$$

where μ is a positive constant, μ can be unknowable.

Based on the definitions and deductions above, a high-order nonlinear disturbance observer is designed as

$$\begin{aligned} \hat{d} &= p_1 + q_1(\phi_1 + \phi_2) \\ \dot{p}_1 &= -q_1(\varphi_1 + \varphi_2) - q_1\hat{d} + \hat{d} \\ \hat{d} &= p_2 + q_2(\phi_1 + \phi_2) \\ \dot{p}_2 &= -q_2(\varphi_1 + \varphi_2) - q_2\hat{d} \end{aligned} \quad (17)$$

Where \hat{d} and $\dot{\hat{d}}$ are estimations of d and its derivative respectively, p_1 and p_2 are auxiliary functions, and q_1, q_2 are positive constants. Compared with other NDOs in literature [27, 28], this kind of observer is more simplified and easy to realize.

Let $D = [d \quad \dot{d}]^T$, then HONDO is reformed to be

$$\begin{cases} \dot{\hat{D}} = p + q(\phi_1 + \phi_2) \\ \dot{p} = -q(\varphi_1 + \varphi_2) + Q\hat{D} \end{cases} \quad (18)$$

where

$$\hat{D} = \begin{bmatrix} \hat{d} \\ \dot{\hat{d}} \end{bmatrix}, \quad p = \begin{bmatrix} p_1 \\ p_2 \end{bmatrix}, \quad q = \begin{bmatrix} q_1 \\ q_2 \end{bmatrix}, \quad Q = \begin{bmatrix} -q_1 & 1 \\ -q_2 & 0 \end{bmatrix}$$

According to (18), the derivative of \hat{D} is yielded as

$$\begin{aligned} \dot{\hat{D}} &= \dot{p} + q(\dot{\phi}_1 + \dot{\phi}_2) \\ &= -q(\varphi_1 + \varphi_2) + Q\hat{D} + q(\varphi_1 + \varphi_2 + d) \\ &= Q\hat{D} + qd \end{aligned} \quad (19)$$

Then the estimation error can be defined as follows

$$\tilde{D} = D - \hat{D} \quad (20)$$

The observer error dynamics can be written as

$$\begin{aligned} \dot{\tilde{D}} &= \dot{D} - \dot{\hat{D}} \\ &= \begin{bmatrix} \dot{d} \\ \ddot{d} \end{bmatrix} - Q\hat{D} + qd \\ &= \left(\begin{bmatrix} 0 & 1 \\ 0 & 0 \end{bmatrix} \begin{bmatrix} d \\ \dot{d} \end{bmatrix} + \begin{bmatrix} 0 \\ 1 \end{bmatrix} \ddot{d} \right) - \\ &\quad \left(Q\hat{D} + \begin{bmatrix} q_1 & 0 \\ q_2 & 0 \end{bmatrix} \begin{bmatrix} d \\ \dot{d} \end{bmatrix} \right) \\ &= Q\tilde{D} + \begin{bmatrix} 0 \\ 1 \end{bmatrix} \ddot{d} \end{aligned} \quad (21)$$

Define $E = [0 \quad 1]^T$, then (21) becomes

$$\dot{\tilde{D}} = Q\tilde{D} + E\ddot{d} \quad (22)$$

Supposing that q_1 and q_2 are chosen to guarantee that the eigenvalues of Q are in the left hand plane, then a positive definite symmetric matrix P can be found to satisfy

$$Q^T P + P Q = -R, \quad (23)$$

for any given positive definite matrix R . Define λ_s to be the smallest eigenvalue of R .

To analysis the stability of HONDO, construct a Lyapunov function as

$$V_2 = \tilde{D}^T P \tilde{D} \quad (24)$$

The derivative of V_2 is get via (23)

$$\begin{aligned} \dot{V}_2 &= \dot{\tilde{D}}^T P \tilde{D} + \tilde{D}^T P \dot{\tilde{D}} \\ &= (Q\tilde{D} + E\ddot{d})^T P \tilde{D} + \tilde{D}^T P (Q\tilde{D} + E\ddot{d}) \\ &\leq -\tilde{D}^T R \tilde{D} + 2 \| \tilde{D} \| \| P E \| \mu \\ &\leq -\| \tilde{D} \| (\lambda_s \| \tilde{D} \| - 2 \| P E \| \mu) \end{aligned} \quad (25)$$

Then, after a relatively long time, the norm of the estimation error is bounded by

$$\| \tilde{D} \| \leq \lambda_1, \quad (26)$$

where

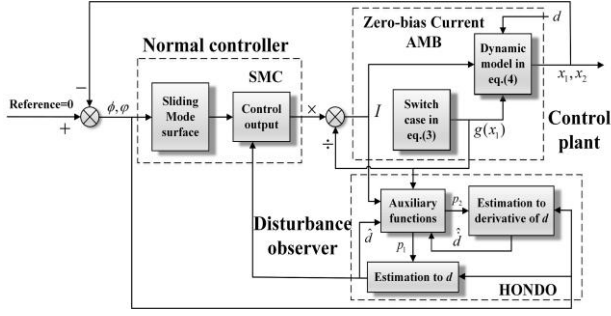


Figure 2. The whole control system of the zero-bias current controlled AMB based on SMC+HONDO.

$$\lambda_1 = \frac{2 \|PE\| \mu}{\lambda_s} \quad (27)$$

Therefore, the norm of the extended disturbance estimation error \tilde{D} is ultimately bounded and the bounds can be lowered by choosing q_1, q_2, P and R appropriately.

Remark 2: The class of disturbances considered here is much larger than the normal nonlinear disturbance observer based design since the derivative of the disturbance is also estimated. Differs from the CNDO in [22], the derivatives of lumped disturbance is no longer restricted to be nearly zero for the HONDO, a common bound μ can be found for the lumped disturbance and its derivatives. Therefore, stronger ability to handle varying disturbance can be expected. Besides, it should be mentioned that the bound μ is unnecessary to know.

Fig. 2 draws the whole control system of the zero-bias current controlled AMB based on the method combining HONDO with SMC. Besides, for the convenience of discussion, the control system adopting HONDO and SMC is abbreviated as SMC+HONDO, similarly, SMC+CNDO for one consists of CNDO and SMC.

D. Simulation

In this section, we apply the SMC+CNDO [22] and the SMC+HONDO to the zero-bias current controlled AMB system separately. Three kinds of conditions, the step response, 360 N step load and 200 N / 20 Hz sine load added to rotor, are taken into consideration. Besides, to make a comparison, the sliding mode control (SMC) and adaptive backstepping sliding mode control (ABSMC) [17] are also implied to the same system.

As shown in (3), $g(x_1)I$ is strongly nonlinear in the vicinity of $x_1 = 0$, which results in serious chatter. Thereby, to reduce chattering, the sign function in (14) is replaced by the following saturated function

$$\text{sgn}(\sigma) \approx \text{sat}(\sigma) = \frac{\sigma}{|\sigma| + \delta}, \quad \delta = \begin{cases} 0, & |\sigma| \geq \eta \\ \delta_0, & |\sigma| < \eta \end{cases} \quad (28)$$

where η, δ_0 are positive constants.

The design parameters are chosen as follows:

- **SMC:** $c=800, k=10, h=800, \eta=0.1, \delta_0=0.1$
- **ABSMC:** $c=100, k=100, h=30, \beta=5, \gamma=50000, \eta=0.01, \delta_0=0.01$
- **SMC+CNDO:** $c=800, k=1, h=800, l=400, \eta=0.004,$

$\delta_0=0.004$

- **SMC+HONDO:** $c=800, k=1, h=800, l_1=1000, l_2=1000, \eta=0.00003, \delta_0=0.00001.$

In Fig. 3, it shows that the rotor suspends at the center within 0.1 s well under a 0.18 mm step reference displacement for the four methods. It demonstrates that the ABSMC has the minimum settling time, while the setting up process for SMC+CNDO is the longest one. Besides, Fig. 3 presents that

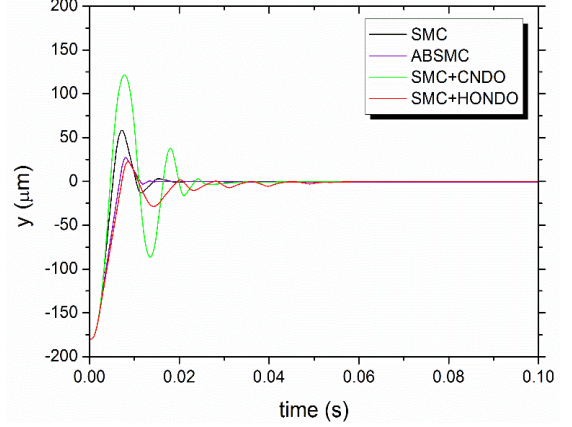


Figure 3. The simulated displacement curves of the step response (initial displacement is -0.18 mm).

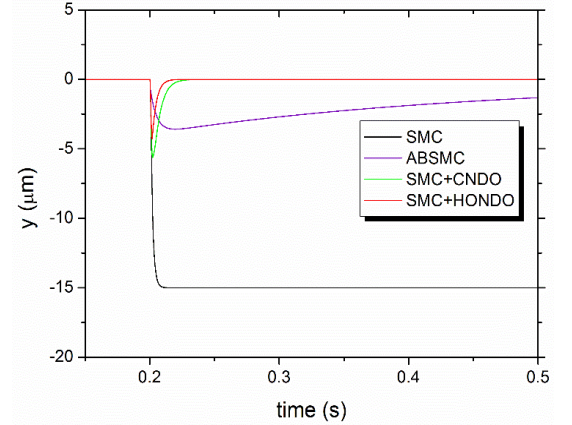


Figure 4. The simulated displacement curves under the 360 N step load.

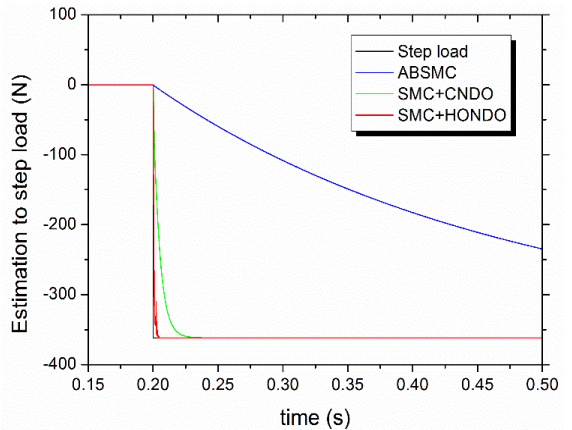


Figure 5. The simulated disturbance estimation curves under the 360 N step load.

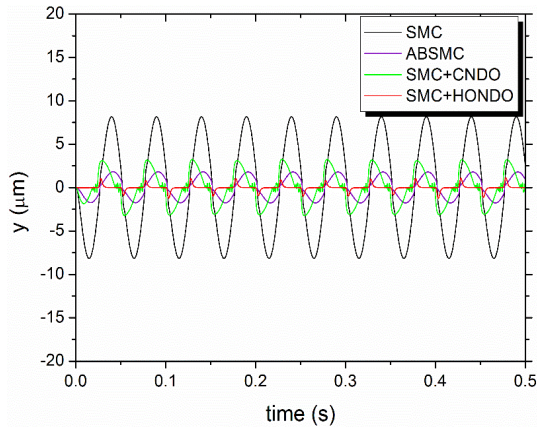


Figure 6. The simulated displacement curves under the 200 N / 20 Hz sine load.

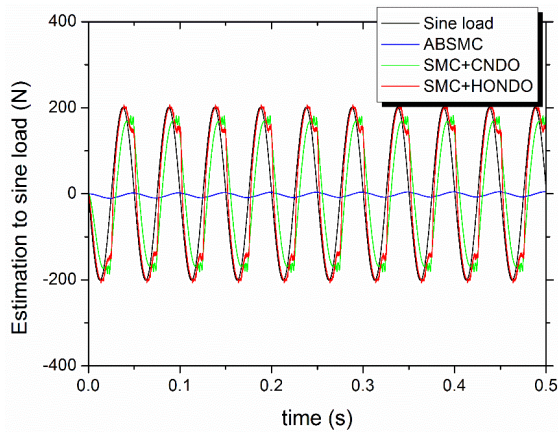


Figure 7. The simulated disturbance estimation curves under the 200 N / 20 Hz sine load.

there exist several oscillations in the displacement curves for the four methods, this is because the switching laws in (3) is at work. The overshoot of displacement curve is the largest one for the SMC+CNDO.

It can be observed from Fig. 4 that with a 360 N step load adding to the rotor, for SMC, a steady displacement from the center is generated which is about $-15 \mu\text{m}$, while a $-3.3 \mu\text{m}$ error at max occurs and then decreases slowly for ABSMC. However, a maximum error of $-5.6 \mu\text{m}$ is formed and then converges to zero within 0.06 s for the SMC+CNDO, and the largest displacement and the adjustment time change to $-4.3 \mu\text{m} / 0.04 \text{ s}$ for the SMC+HONDO method. Moreover, the curves of estimation to the step load for the methods except SMC are shown in Fig. 5. We can conclude that the SMC method is short of handling disturbance with unknown bound, and though there is an adaptive law to estimate the disturbance in the ABSMC algorithm, the estimating rate is slow. The disturbance observer based control approach has faster estimating rate than the conventional methods with inner adaptive law. Moreover, the HONDO tracks the step load more quickly than the CNDO. This corresponds well to the analysis in above sections.

From Fig. 6, we can conclude that the rotor vibrates around the center at 20 Hz when adds the sine load to the rotor. The sine load is supposed to be generated by the parameter variation. The vibration amplitudes are about $8.2 \mu\text{m}$ for SMC, $1.8 \mu\text{m}$ for

ABSMC, $3.1 \mu\text{m}$ for SMC+CNDO, and under $1.1 \mu\text{m}$ for SMC+HONDO separately. Fig. 7 shows that the HONDO tracks the sine load well, while there remains small error and time delay in the estimation curve for the CNDO, and the adaptive law in the ABSMC algorithm is almost disabled to estimate the sine load. The results are consistent with above analysis. The HONDO is good at handling different kinds of disturbance. Therefore, the effectiveness of the high-order disturbance observer is proven.

Therefore, in the simulation part, excellent performance can be shown for the SMC+HONDO method under different kinds of conditions.

E. Experiment

Fig. 8 shows the structure of the experiment platform researched in this paper. Fig. 8(a) and Fig. 8(b) represent the construction of a power magnetically levitated spindle (PMLS) system, which is made of a radial AMB, an axial AMB, a bearingless motor and a loading plant mainly. The radial AMB is the primary part to bear external load in the radial directions. Since that, the proposed methods are applied to the radial AMB. The whole control system consists of the signal processing part, the control board, the power board and the AC-DC inverter mainly. The SMC, ABSMC, SMC+CNDO, SMC+HONDO algorithms are realized in a FPGA chip, the EP4CE15F256 FPGA manufactured by ALTERA is utilized. These proposed control methods employ the cascaded structure with position and current feedback. The inner current loop adopts the hysteretic current control to realize the fast response of current. The mass of the rotor is 34.2 kg, the magnetic force coefficient is $4.5 \times 10^{-5} \text{ N} \cdot \text{m}^2 / \text{A}^2$, the nominal air gap is 0.5 mm, the turns of coils are chosen as 280.

Corresponds to the simulation section, the four methods are realized for the zero-bias current controlled AMB system

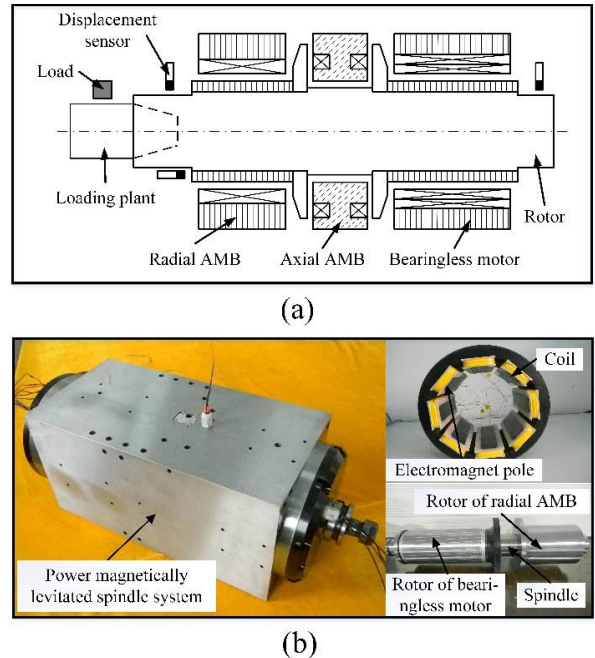


Figure 8. Structure of the experiment platform: (a) the construction model of a power magnetically levitated spindle (PMLS) system, (b) the configuration of the PMLS system and radial magnetic bearing.

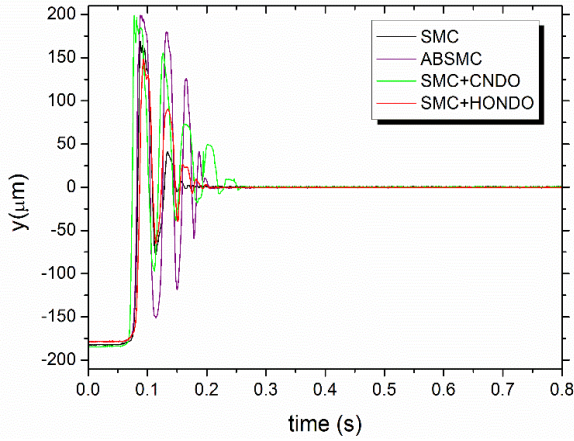


Figure 9. The experimental displacement curves of the step response (initial displacement is about -0.18 mm).

respectively for different conditions. The following discussions focus on the vertical DOF of the radial AMB.

From Fig. 9, it can be concluded that both the four methods can make the rotor suspend at the center from -0.18 mm initial displacement within 0.3 s. It costs 0.16s, 0.20 s, 0.24 s, 0.18 s to reach the steady state for the SMC, ABSMC, SMC+CNDO, and SMC+HONDO respectively. Similar to the simulation results, several oscillations can be seen in the displacement curve for the four methods. Different from the simulation results, faster response is shown for SMC+HONDO than ABSMC.

Fig. 10 shows that similar to the simulation result, when adds a 360 N step load to the rotor at about $t = 0.05$ s, a steady displacement from the center of which the value is about -29.5 μm and the adjusting time is about 0.11 s for the SMC method, a max error of -3.7 μm occurs and then stabilizes at -2.0 μm for the ABSMC method, and the setting up process costs about 0.3 s. While, for the disturbance observer based designs, an overshoot of about -6 μm is produced and quickly converges to zero within 0.1 s for the SMC+CNDO, and the max error and settling time are -4.7 μm and 0.08 s for the SMC+HONDO.

Then an assumption is made that the magnetic force coefficient K is varying with an error of 50 % and the frequency is 20 Hz, and Fig. 11 shows the displacement curves of rotor for the four approaches. It clearly shows that the SMC+HONDO

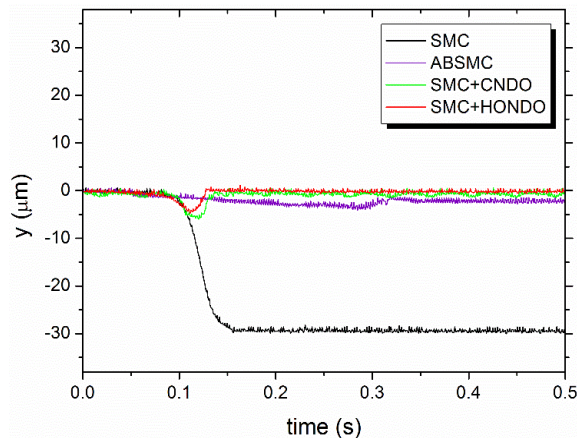


Figure 10. The experimental displacement curves under the 360 N step load.

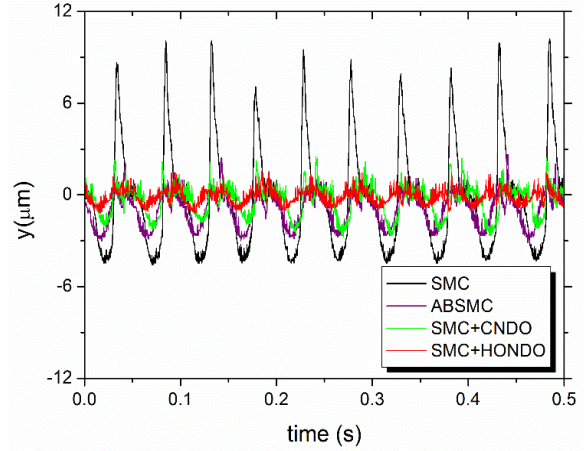


Figure 11. The experimental displacement curves with 50 % / 20 Hz varied magnetic force coefficient K .

has the best performance to handle the changed disturbance with the vibrating amplitude of under 1.4 μm , while the value of amplitudes for SMC+CNDO, ABSMC, SMC are 2.7 μm , 3 μm , 10.5 μm respectively. Therefore, the SMC+HONDO method performs better in resisting the lumped disturbance than the others.

From above, it demonstrates that the disturbance observer based methods have stronger ability to resist disturbance than the baseline control method and method with an inner adaptive law, while maintaining the nominal performance with identical suspending precision. Moreover, the experiment results when adding disturbance obviously verify that the HONDO is more effective than the CNDO, as the derivative of the disturbance is estimated at the same time. Therefore, the validity of the high-order disturbance observer is proven.

F. Conclusions

In this paper, the undeterminable lumped disturbance rejection problem in a new zero-bias current controlled AMB system is investigated. The zero-bias current controlled way is proposed to realize the power-minimizing control for AMB system. First, the construction of the lumped disturbance is analyzed and a new zero-bias current controlled AMB model is built. Then the conventional nonlinear disturbance observer and high-order nonlinear disturbance observer are discussed separately, and the disturbance observer based sliding mode controller designs are presented. The high-order nonlinear disturbance observer estimates the disturbance and its derivative at the same time, while the conventional nonlinear disturbance observer assumes that the derivative of disturbance equals to zero. Both simulation and experiment results show that the feasibility of the proposed algorithm. Besides, the high-order nonlinear disturbance observer based sliding mode controller is compared with the baseline sliding mode controller without disturbance observer, the adaptive backstepping sliding mode controller and the conventional nonlinear disturbance observer based design. The results show the superiority both in maintaining nominal performance and disturbance rejection for the proposed high-order nonlinear disturbance observer based controller than other methods. Since the time-varying disturbance widely exists in practice, better performance can be

expected for the power-minimizing controlled AMB with the proposed approach.

REFERENCES

- [1] Schweitzer G, Larssonneur R, Traxler A, et al, "Magnetic Bearings," *International Centre for Mechanical Sciences*, vol. 297, pp. 543–570, 1989.
- [2] Tsai N C, Lee R M, "Regulation of spindle position by magnetic actuator array," *Journal of Advanced Manufacturing Technology*, vol. 53, no. 1–4, pp. 93–104, 2011.
- [3] Tsai N C, Shih L W, Lee R M, "Position regulator for spindle of milling machine by embedded magnetic bearings," *Journal of Intelligent Manufacturing*, vol. 22, no. 4, pp. 563–574, 2011.
- [4] Peng C, Fang J, Xu S, "Composite anti-disturbance controller for magnetically suspended control moment gyro subject to mismatched disturbances," *Nonlinear Dynamics*, vol. 79, no. 2, pp. 1563–1573, 2015.
- [5] Jiang W, Zhou K, Lv J, et al, "Superconducting EMS feed drive system of NC machine tool," *The International Journal of Advanced Manufacturing Technology*, vol. 74, no. 5–8, pp. 1053–1060, 2014.
- [6] Sivrioglu S, "Adaptive backstepping for switching control active magnetic bearing system with vibrating base," *IET Control Theory & Applications*, vol. 1, no. 4, pp. 1054–1059, 2007.
- [7] Jastrze R P, Pöllänen R, "Compensation of nonlinearities in active magnetic bearings with variable force bias for zero-and reduced-bias operation," *Mechatronics*, vol. 19, no. 5, pp. 629–638, 2009.
- [8] Jastrzebski R P, Smirnov A, Mystkowski A, et al, "Cascaded position-flux controller for an AMB system operating at zero bias," *Energies*, vol. 7, no. 6, pp. 3561–3575, 2014.
- [9] Sahinkaya M N, Hartavi A E, "Variable bias current in magnetic bearings for energy optimization," *IEEE Transactions on Magnetics*, vol. 43, no. 3, pp. 1052–1060, 2007.
- [10] Tsiotras P, Arcak M, "Low-bias control of AMB subject to voltage saturation: State-feedback and observer designs," *IEEE Transactions on Control Systems Technology*, vol. 13, no. 2, pp. 262–273, 2005.
- [11] Gao W, Hung J C, "Variable structure control of nonlinear systems: A new approach," *IEEE transactions on Industrial Electronics*, vol. 40, no. 1, pp. 45–55, 1993.
- [12] Huang Y S, Sung C C, "Implementation of sliding mode controller for linear synchronous motors based on direct thrust control theory," *IET control theory & applications*, vol. 4, no. 3, pp. 326–338, 2010.
- [13] Kang M S, Lyou J, Lee J K, "Sliding mode control for an active magnetic bearing system subject to base motion," *Mechatronics*, vol. 20, no. 1, pp. 171–178, 2010.
- [14] Zhang H, Liu X, Wang J, et al, "Robust H_∞ sliding mode control with pole placement for a fluid power electrohydraulic actuator (EHA) system," *The International Journal of Advanced Manufacturing Technology*, vol. 73, no. 5–8, pp. 1095–1104, 2014.
- [15] Carneiro J F, de Almeida F G, "Accurate motion control of a servopneumatic system using integral sliding mode control," *The International Journal of Advanced Manufacturing Technology*, vol. 77, no. 9–12, pp. 1533–1548, 2015.
- [16] Lee J D, Khoo S, Wang Z B, "DSP-based sliding-mode control for electromagnetic-levitation precise-position system," *IEEE Transactions on Industrial Informatics*, vol. 9, no. 2, pp. 817–827, 2013.
- [17] Lin F J, Chang C K, Huang P K, "FPGA-based adaptive backstepping sliding-mode control for linear induction motor drive," *IEEE Transactions on power electronics*, vol. 22, no. 4, pp. 1222–1231, 2007.
- [18] Song Z, Sun K, "Adaptive backstepping sliding mode control with fuzzy monitoring strategy for a kind of mechanical system," *ISA transactions*, vol. 53, no. 1, pp. 125–133, 2014.
- [19] Chen W H, "Disturbance observer based control for nonlinear systems," *IEEE/ASME transactions on mechatronics*, vol. 9, no. 4, pp. 706–710, 2004.
- [20] Yang J, Zolotas A, Chen W H, et al, "Robust control of nonlinear MAGLEV suspension system with mismatched uncertainties via DOBC approach," *ISA transactions*, vol. 50, no. 3, pp. 389–396, 2011.
- [21] Yang J, Li S, Yu X, "Sliding-mode control for systems with mismatched uncertainties via a disturbance observer," *IEEE Transactions on industrial electronics*, vol. 60, no. 1, pp. 160–169, 2013.
- [22] Mohammed S, Huo W, Huang J, et al, "Nonlinear disturbance observer based sliding mode control of a human-driven knee joint orthosis," *Robotics and Autonomous Systems*, vol. 75, pp. 41–49, 2016.
- [23] Wang Z, Wu Z, "Nonlinear attitude control scheme with disturbance observer for flexible spacecrafts," *Nonlinear Dynamics*, vol. 81, no. 1–2, pp. 257–264, 2015.
- [24] Lee D, "Nonlinear disturbance observer-based robust control of attitude tracking of rigid spacecraft," *Nonlinear Dynamics*, vol. 88, no. 2, pp. 1317–1328, 2017.
- [25] Ginoya D, Shendge P D, Phadke S B, "Disturbance observer based sliding mode control of nonlinear mismatched uncertain systems," *Communications in Nonlinear Science and Numerical Simulation*, vol. 26, no. 1–3, pp. 98–107, 2015.
- [26] Yao X, Guo L, "Composite anti-disturbance control for Markovian jump nonlinear systems via disturbance observer," *Automatica*, vol. 49, no. 8, pp. 2538–2545, 2013.
- [27] Kim K S, Rew K H, Kim S, "Disturbance observer for estimating higher order disturbances in time series expansion," *IEEE Transactions on automatic control*, vol. 55, no. 8, pp. 1905–1911, 2010.
- [28] Yang J, Su J, Li S, et al, "High-order mismatched disturbance compensation for motion control systems via a continuous dynamic sliding-mode approach," *IEEE Transactions on Industrial Informatics*, vol. 10, no. 1, pp. 604–614, 2014.
- [29] Ginoya D, Shendge P D, Phadke S B, "Sliding mode control for mismatched uncertain systems using an extended disturbance observer," *IEEE Transactions on Industrial Electronics*, vol. 61, no. 4, pp. 1983–1992, 2014.
- [30] Xiao L, Zhu Y, "Sliding mode output feedback control based on tracking error observer with disturbance estimator," *ISA transactions*, vol. 53, no. 4, pp. 1061–1072, 2014.